APPLIED AND ENVIRONMENTAL MICROBIOLOGY, June 2010, p. 3999–4007 Vol. 76, No. 12
0099-2240/10/$12.00 doi:10.1128/AEM.00027-10

Purification and Characterization of OmcZ, an Outer-Surface, Octaheme *c*-Type Cytochrome Essential for Optimal Current Production by *Geobacter sulfurreducens*▽†

Kengo Inoue,[1,2]* Xinlei Qian,[1] Leonor Morgado,[3] Byoung-Chan Kim,[1] Tünde Mester,[1] Mounir Izallalen,[1] Carlos A. Salgueiro,[3] and Derek R. Lovley[1]

Department of Microbiology, University of Massachusetts, Amherst, Massachusetts 01003[1]; Interdisciplinary Research Organization, University of Miyazaki, Miyazaki, Japan[2]; and Requimte-CQFB, Departamento Química, Faculdade de Ciências e Tecnologia, Universidade Nova de Lisboa, Campus Caparica, Portugal[3]

Received 5 January 2010/Accepted 8 April 2010

Previous studies have demonstrated that *Geobacter sulfurreducens* requires the *c*-type cytochrome OmcZ, which is present in large ($OmcZ_L$; 50-kDa) and small ($OmcZ_S$; 30-kDa) forms, for optimal current production in microbial fuel cells. This protein was further characterized to aid in understanding its role in current production. Subcellular-localization studies suggested that $OmcZ_S$ was the predominant extracellular form of OmcZ. N- and C-terminal amino acid sequence analysis of purified $OmcZ_S$ and molecular weight measurements indicated that $OmcZ_S$ is a cleaved product of $OmcZ_L$ retaining all 8 hemes, including 1 heme with the unusual *c*-type heme-binding motif $CX_{14}CH$. The purified $OmcZ_S$ was remarkably thermally stable (thermal-denaturing temperature, 94.2°C). Redox titration analysis revealed that the midpoint reduction potential of $OmcZ_S$ is approximately −220 mV (versus the standard hydrogen electrode [SHE]) with nonequivalent heme groups that cover a large reduction potential range (−420 to −60 mV). $OmcZ_S$ transferred electrons *in vitro* to a diversity of potential extracellular electron acceptors, such as Fe(III) citrate, U(VI), Cr(VI), Au(III), Mn(IV) oxide, and the humic substance analogue anthraquinone-2,6-disulfonate, but not Fe(III) oxide. The biochemical properties and extracellular localization of OmcZ suggest that it is well suited for promoting electron transfer in current-producing biofilms of *G. sulfurreducens*.

The properties of proteins involved in the production of current in microbial fuel cells are of interest because it seems likely that the applications of microbial fuel cells could be further optimized and expanded if the mechanisms for current production were better understood. *Geobacter sulfurreducens* produces current densities that are among the highest of any known microorganism (40, 59) and is closely related to the microorganisms that most effectively colonize the anodes of microbial fuel cells from a diversity of complex microbial communities (4, 18–20, 24–27, 53).

A comparison of gene expression in current-producing biofilms of *G. sulfurreducens* growing on the graphite anodes of microbial fuel cells versus gene expression in biofilms growing on the same material but with fumarate as the electron acceptor demonstrated that transcript abundance for the gene for the outer-surface *c*-type cytochrome OmcZ was much higher in the current-producing cells (39). Deletion of *omcZ* greatly inhibited current production (39) and increased the resistance in electron transfer between the biofilm and the anode surface (48). *G. sulfurreducens* has an abundance of other outer-surface *c*-type cytochromes that are important in other forms of extracellular electron transfer, such as the reduction of Fe(III) (25, 37), U(VI) (49), or humic substances (58), and some may play an important electron storage role (13), but OmcZ is the only *c*-type cytochrome that was found to be essential for optimal current production (39).

Previous proteome analyses had revealed that most of the more than 100 putative *c*-type cytochrome genes in *G. sulfurreducens* are expressed (11, 12). However, only a few of them have been purified and characterized. They include PpcA, an abundant triheme periplasmic *c*-type cytochrome that plays an important role in Fe(III) reduction (28, 38, 43), as well as several monoheme cytochromes that may play a sensory role (22, 44, 45). None of the outer-surface *c*-type cytochromes has been purified to homogeneity. A *c*-type cytochrome preparation, designated FerA, was found to contain components of the NADH dehydrogenase Fe(III)-reducing protein complex (34, 35) and had the capacity to reduce Fe(III). It was later concluded that FerA was probably a mixture of the multiheme cytochrome homologues OmcB and OmcC (25). Gene deletion studies demonstrated that OmcB is required for optimal Fe(III) reduction but OmcC is not (24, 25). Thus, there is a dearth of information on the biochemistry of outer-surface cytochromes of *G. sulfurreducens*. Studies with *Shewanella oneidensis* have demonstrated the importance of purifying and characterizing outer-surface cytochromes in order to understand the mechanisms for extracellular electron transfer (50, 51). Here, we report on the isolation and characterization of OmcZ from *G. sulfurreducens*.

MATERIALS AND METHODS

Bacterial strains and culture conditions. *Geobacter sulfurreducens* strain ZKI was produced from *G. sulfurreducens* strain DL-1 as described by B.-C. Kim

* Corresponding author. Mailing address: Department of Microbiology, University of Massachusetts, 639 North Pleasant St., Amherst, MA 01003. Phone: (413) 577-2440. Fax: (413) 577-4660. E-mail: kinoue@microbio.umass.edu.

† Supplemental material for this article may be found at http://aem.asm.org/.

▽ Published ahead of print on 16 April 2010.

(unpublished data). Briefly, the *omcZ* gene, combined with 500 bp containing the *ompJ* promoter sequence, was integrated in strain DL-1. Strain ZKI, which overproduces the *omcZ* gene product, was used for OmcZ small-form ($OmcZ_S$; 30-kDa) purification. Strains DL-1 and ZKI and an *omcZ*-deficient mutant (39) were cultured anaerobically in acetate-fumarate medium as previously described (8).

Preparation of subcellular fractions. Subcellular fractions were prepared using modifications of previously described methods (9, 21, 41). Wild-type and strain ZKI cells in their mid-log and stationary growth phases in 100 ml of acetate-fumarate medium were harvested by centrifugation for 15 min at 6,000 × *g* at 4°C. The supernatants were reserved as the culture supernatant fraction. The harvested cells were washed with 50 ml of spheroplast wash medium consisting of 0.42 g/liter KH_2PO_4, 0.22 g/liter K_2HPO_4, 0.38 g/liter KCl, 4.96 g/liter NaCl, 1.8 g/liter $NaHCO_3$, and 0.5 g/liter Na_2CO_3. The washed cells were pelleted by centrifugation for 6 min at 6,000 × *g* at 4°C and resuspended in 30 ml of spheroplast wash medium containing 350 mM sucrose. Following another centrifugation for 6 min at 6,000 × *g* at 4°C, the cells were resuspended in 10 ml of 250 mM Tris-HCl (pH 7.5). After 1 min of incubation at 30°C, 1 ml of 500 mM EDTA (pH 7.5) was added, followed by the addition of 10 ml of 700 mM sucrose at 2 min, 150 mg lysozyme at 3.5 min, and 20 ml of water at 4 min. Spheroplast formation in the suspension was confirmed by transmission electron microscopy (negatively stained whole mounts). After centrifugation for 10 min at 20,000 × *g* at 4°C to pellet the spheroplasts, the supernatant was reserved as the periplasmic fraction. The pellet was resuspended in 20 ml of 100 mM Tris-HCl buffer (pH 7.5). A few crystals of DNase I were added, and the spheroplasts were disrupted by sonication for 5 min on ice (Sonic Dismembrator F550; Fisher Scientific). The resulting crude extract was centrifuged for 30 min at 3,000 × *g* at 4°C. The pellet was reserved as the cell debris fraction. The supernatant was subsequently centrifuged for 30 min at 20,000 × *g* at 4°C. The supernatant was reserved as the cytoplasmic fraction. The pellet was resuspended in 4 ml of 100 mM Tris-HCl buffer (pH 7.5). Following the addition of 4 ml of 100 mM Tris-HCl (pH 7.5) containing 2% (wt/vol) lauroylsarcosine, the suspension was stirred for 15 min at room temperature and then centrifuged for 30 min at 125,000 × *g* at 4°C. The supernatant was reserved as the inner membrane fraction. The pellet was resuspended in 200 μl of 100 mM Tris-HCl buffer (pH 7.5) and reserved as the outer membrane fraction. All the fraction samples were concentrated, and their buffer was replaced with 100 mM Tris-HCl (pH 7.5) by ultrafiltration with Amicon Ultra-15 Centrifugal Filter Units (10,000 MW; Millipore) or Nanosep 10k Omega (Pall).

Purification of $OmcZ_S$ from strain ZKI. All purification steps were performed at room temperature. *G. sulfurreducens* strain ZKI was anaerobically grown in six 1.5-liter volumes of acetate-fumarate medium (8) to stationary phase at 30°C. The cells were harvested and resuspended in Tris-HCl buffer (50 mM Tris-HCl, pH 7.0). After disruption by freeze-thaw 3 times, the pellet was collected as an insoluble fraction by centrifugation at 6,000 × *g* for 15 min at room temperature and suspended in 200 ml of Tris-HCl buffer, followed by centrifugation at 12,000 × *g* for 10 min. The pellet was washed twice with 120 ml of 50 mM Tris-HCl containing 1% SDS and suspended in 60 ml of 50 mM Tris-HCl buffer, and 60 ml of 10% 3-(*N*,*N*-dimethylmyristyl-ammonio)propanesulfonate (Zwittergent 3-14) solution was added. The insoluble fraction was collected by centrifugation and suspended in 10 ml of 10% Zwittergent 3-14 solution. After centrifugation at 12,000 × *g* for 10 min, the red supernatant was collected and diluted to 1:4 with 50 mM Tris-HCl buffer. The red material containing $OmcZ_S$ was precipitated by centrifugation at 12,000 × *g* for 10 min because of its insolubility in highly concentrated Tris-HCl buffer. At this step, $OmcZ_S$ was the only protein in the precipitant identified on the SDS-PAGE gel. The OmcZ large form ($OmcZ_L$; 50 kDa) was not detected in the precipitant because the ZKI stationary-phase cells contain very little $OmcZ_L$, which is more soluble than $OmcZ_S$ according to the subcellular fractioning. The pellet was resuspended in 10 ml of 1% SDS solution and incubated at 90°C for 5 min, followed by filtration with Nanosep 300k Omega (Pall). To remove SDS, the solvent of the filtered solution was replaced in 5 mM Tris-HCl buffer by ultrafiltration using Nanosep 10k Omega (Pall). $OmcZ_S$ was purified by gel filtration chromatography using a fast protein liquid chromatography (FPLC) system (Pharmacia Biotech), a HiPrep Sephacryl S-200 HR column (GE Healthcare), and buffer containing 50 mM Tris-HCl (pH 7.0) and 0.1 mM NaCl. Fractions containing $OmcZ_S$ were collected and concentrated with a Vivaspin 20 (10-kDa cutoff; Sartorius).

Protein quantification, SDS-PAGE, and Western blotting. Protein concentrations were determined by the Bradford method with bovine serum albumin (BSA) as a standard (6), using Quick Start Bradford Dye Reagent (Bio-Rad). For outer membrane and inner membrane fractions, cell debris protein concentrations were measured by the bicinchoninic acid method (52). For outer membrane and cell debris fractions, protein concentrations were determined after the proteins were boiled with SDS (0.5% final concentration) for 10 min to solubilize them as much as possible. SDS-PAGE analyses were performed using 12.5% (wt/vol) polyacrylamide gels. Proteins were stained with Coomassie brilliant blue R-250 and were heme stained as previously described (14, 56) for identification of *c*-type cytochromes. SeeBlue Plus2 Pre-Stained Standard (Invitrogen) was used as a protein molecular mass standard. Western blotting was performed using polyvinylidene difluoride (PVDF) membranes and a One-Step Western Blot Kit (GenScript), according to the manufacturer's instructions. Polyclonal antibodies to OmcZ were produced against purified $OmcZ_S$ in New Zealand White rabbits (New England Peptide). The antibody against $OmcZ_S$ was purified by using blotted antigen. The purified $OmcZ_S$ was separated by SDS-PAGE and blotted to a PVDF membrane using a semidry blotter. A portion of the blot containing $OmcZ_S$ was cut and washed with TBST buffer (20 mM Tris-HCl [pH 7.5], 0.5 M NaCl, and 0.05% Tween 20). The portion was blocked with 3% (wt/vol) BSA in TBST buffer for 30 min, followed by washing with TBST buffer, and was soaked in crude serum with antibody to $OmcZ_S$. After incubation for 4 h, the portion was washed with TBST buffer 3 times. The antibody bound to the portion was eluted with 0.1 M glycine-HCl (pH 2.7) buffer. The eluted antibody was neutralized with 1/5 the volume of 1 M Tris-HCl (pH 7.5). The purified antibody was used at 1:1,000 dilution. The Western blots were scanned and digitized with NIH Image J software for the subcellular-localization analysis of $OmcZ_L$ and $OmcZ_S$. The integrated pixel densities (the pixel density of a band after background subtraction) of $OmcZ_L$ and $OmcZ_S$ were used as the intensities for calculation. The percentage of $OmcZ_L$ or $OmcZ_S$ molecules that was present in each subcellular fraction was calculated. The total relative amount of $OmcZ_L$ or $OmcZ_S$ in each subcellular fraction was calculated by multiplying the ratio of the total protein in each fraction to the amount of the protein loaded in each well of the gel. This multiplied intensity gave the relative amount of $OmcZ_L$ or $OmcZ_S$ in that fraction. The multiplied intensity of a fraction—for example, the cytoplasmic fraction—was divided by the total of the multiplied intensities of all the fractions (cytoplasmic, inner membrane, periplasmic, outer membrane, and culture supernatant fractions), which gave the relative localization ratio of the cytoplasmic fraction. The localization ratios of the other subcellular fractions were calculated in the same manner. The localization ratios provided qualitative rather than quantitative relative amounts in the different subcellular fractions. The loosely bound outer membrane-enriched protein fractions (LBOP) of the cells were prepared as previously described (37).

N-terminal, internal, and C-terminal sequence determination. The N terminus sequence data were obtained by Edman sequencing at the Rockefeller University Protein/DNA Technology Center. The C terminus sequence data of $OmcZ_S$ were obtained at Commonwealth Biotechnologies, Inc., by a method using carboxypeptidase. Carboxypeptidase Y and the Amino Quant high-performance liquid chromatography (HPLC) system (Agilent) were used for enzymatic degradation and amino acid quantification, respectively. To obtain internal sequence data, the purified $OmcZ_S$ bands in SDS-PAGE gels were excised and sent to the Laboratory for Proteomic Mass Spectrometry at the University of Massachusetts Medical School for tryptic digestion, followed by liquid chromatography-tandem mass spectrometry (LC–MS-MS) analysis.

Molecular mass determination for $OmcZ_S$. The relative molecular mass of $OmcZ_S$ was estimated by gel filtration chromatography using an MW-GF-200 kit (Sigma). Mass spectra from electrospray ionization (ESI)-MS were acquired on a QStar-XL hybrid quadrupole time-of-flight mass spectrometer (ABI/MDS-Sciex), equipped with an ESI source. Purified $OmcZ_S$ was dissolved in a mixture of water, ethanol, and acetic acid (50:50:3 [vol/vol/vol]) and was analyzed by ESI-MS. Analysis was also conducted on $OmcZ_S$ dissolved in 10 mM ammonium bicarbonate. Voltages were adjusted to obtain the best ion transmission of *m*/*z* 3,000 corresponding to the protein. An MS scan (*m*/*z* 500 to 2,200) was performed in the positive ion acquisition mode.

Spectroscopic analysis. UV/visible-light absorption spectrum measurements were performed using a Cary 50 Bio UV-visible spectrophotometer (Varian) in the range of 275 to 650 nm. The reduced $OmcZ_S$ samples were obtained by adding 5 μl of 100 mM dithiothreitol (DTT) to the oxidized samples. CD spectra were recorded in the far-UV region using a Jasco J-715 spectropholarimeter at room temperature. A 2-mg/ml purified $OmcZ_S$ sample in water was measured using a cuvette with a path length of 0.01 cm. Cytochrome *c* from horse heart (Sigma) was used as a spectrum standard for *c*-type cytochrome analysis. The proportions of the helices, sheets, and turns were calculated using CDNN version 2.1 (3).

Heme quantification. Pyridine hemochrome analysis was performed as previously described (2). After the addition of NaOH and pyridine (final concentrations, 75 mM and 2.1 M, respectively), the oxidized form of the protein was obtained by the addition of 10 μl of 150 mM potassium ferricyanide solution. The spectrum was recorded, and the protein was then reduced by the addition of 1 M

DTT until no further increase was observed at 550 nm. The heme *c* content of the purified $OmcZ_S$ was calculated using the difference millimolar extinction coefficient of 19.1 mM^{-1} cm^{-1} at 550 nm for the pyridine ferrohemochrome minus the pyridine ferrihemochrome (1).

Thermal stability measurement. The thermal stability of $OmcZ_S$ was investigated by differential scanning calorimetry (DSC) using a VP-DSC/ETR (Microcal). A sample (0.5 mg/ml) in 10 mM sodium phosphate buffer (pH 7.0) was placed in the sample cell, and the same buffer was placed in the reference cell. The DSC scan was run at a rate of 1°C/min.

Determination of redox potential. Redox titrations of the isolated form of $OmcZ_S$ were followed by visible spectroscopy inside an anaerobic glove box kept at <1 ppm oxygen. As previously described (29), the protein solutions (~0.16 mg/ml) were in 32 mM phosphate buffer with NaCl (100 mM final ionic strength) at pH 7 and 298 K. Each redox titration was performed in both the oxidative and reductive directions, using sodium dithionite and potassium ferricyanide solutions as the reductant and oxidant, respectively. To ensure a good equilibrium between the redox centers and the working electrode, a mixture of the following redox mediators was added to the solution, all at approximately 1.5 μM final concentration: phenazine methosulfate, phenazine ethosulfate, gallocyanine, methylene blue, indigo tetrasulfonate, indigo trisulfonate, indigo disulfonate, 2-hydroxy-1,4-naphtoquinone, antraquinone-2,6-disulfonate, antraquinone-2-sulfonate, safranine 0, neutral red, benzyl viologen, diquat, and methyl viologen. These mediators covered the potential range of −440 to +80 mV. The $OmcZ_S$ reduced fraction was determined by integrating the area of the α-band above the line connecting the flanking isobestic points (544 and 561 nm) to subtract the optical contribution of the redox mediators, as previously described (42).

Reduction of metals and AQDS by $OmcZ_S$. The range of electron acceptors reduced by $OmcZ_S$ was determined with a spectrophotometric assay. The purified $OmcZ_S$ (55.4 μg) was dissolved in 0.9 ml of Tris-HCl (pH 7.0) and anaerobically reduced with 5 μl of 100 mM DTT. The spectrum of the DTT-reduced $OmcZ_S$ was recorded between 275 nm and 650 nm. Ten microliters of the potential electron acceptor was added from 100 mM anoxic stock solutions of Fe(III) citrate, potassium chromate, Au(III) chloride trihydrate, or anthraquinone-2,6-disulfonate (AQDS); a 20 mM stock solution of U(VI) acetate; or a suspension of Mn(IV) oxide or Fe(III) oxide at 100 mM per liter (7, 33).

Amino acid sequence analyses. The PSORT algorithm (http://psort.ims.u-tokyo.ac.jp) and SignalP 3.0 Server (http://www.cbs.dtu.dk/services/SignalP) were used to predict the cell localization and signal peptide cleavage sites of the OmcZ protein. The SOSUI engine ver. 1.11 (http://bp.nuap.nagoya-u.ac.jp/sosui) and TMHMM server ver. 2.0 (http://www.cbs.dtu.dk/services/TMHMM-2.0) were used to predict the transmembrane region in the OmcZ protein.

RESULTS AND DISCUSSION

Analysis of the OmcZ sequence. The *omcZ* gene (GSU2076; GenBank accession no. AAR35452) encodes a protein of 473 amino acids with 7 typical heme *c*-binding motifs (CXXCH), as well as the possible heme-binding sequence $CX_{14}CH$ (Fig. 1). The program PSORT predicted OmcZ to be localized in the outer membrane (score, 0.39; certainty, 0.743). The topology prediction programs SOSUI and TMHMM suggested that the N-terminal region (amino acids 5 to 27) forms a transmembrane helix. According to the SignalP server 3.0, OmcZ has a signal sequence with a predicted cleavage site between amino acids 24 and 25 in the transmembrane helix. The cleaved polypeptide, which consists of 449 residues, contains no transmembrane site.

No close OmcZ homologues from outside the genus *Geobacter* were found in the GenBank database. The amino acid sequence of OmcZ had the following percent identities to *Geobacter* proteins: 50.3 to GSU1334 from *G. sulfurreducens* (GenBank accession no. AAR34710), 46.2 to Gbem_3056 from *Geobacter bemidjiensis* strain Bem (ACH40058), 45.6 to GM21_1194 from *Geobacter* sp. strain M21 (EDV70209), and 44.5 to Gmet_0930 from *Geobacter metallireducens* strain GS-15 (ABB31172). The unusual heme-binding motif $CX_{14}CH$ was completely conserved in GM21_1194 and Gbem_3056 and was also conserved with shorter distances between the cysteine residues in GSU1334 ($CX_{13}CH$) and Gmet_0930 ($CX_{11}CH$) (Fig. 1). From amino acid 350 to the C terminus, OmcZ showed homology with the D domain of cyclodextrin glycosyltransferases from *Bacillus* spp. The D domain is well conserved among the cyclodextrin glycosyltransferases, but the function of the domain is still unknown (46).

Subcellular localization of OmcZ. It was previously reported that the loosely bound outer membrane fraction from *G. sulfurreducens* contained two forms of OmcZ with masses of approximately 50 and 30 kDa on SDS-PAGE gels (39). The large and the small forms were designated $OmcZ_L$ and $OmcZ_S$, respectively.

$OmcZ_S$ was more abundant than $OmcZ_L$ in wild-type cells and in strain ZKI, which had been engineered to overexpress OmcZ (Fig. 2). In wild-type cells, both forms of OmcZ were detected in the outer membrane fraction and culture supernatant, but only $OmcZ_S$ was detected in the cell debris fraction, which primarily contained insoluble extracellular matrix material (Fig. 2A). More $OmcZ_S$ was found in the supernatant and cell debris fractions of stationary-phase cells than in mid-log-phase cells. To evaluate the relative amounts of protein in the fractions, the signal intensities of the bands of the Western blots were multiplied by the total amount of protein in each fraction. This analysis indicated that $OmcZ_S$ was most abundant in the cell debris fraction regardless of the growth phase (data not shown). When OmcZ was overexpressed in strain ZKI, some $OmcZ_L$ was also detected in the periplasm of mid-log-phase cells, but $OmcZ_S$ was not (Fig. 2A and B). In both mid-log- and stationary-phase cells, $OmcZ_S$ was mainly distributed in the cell debris fraction and partially in the outer membrane fraction (Fig. 2B and C).

These results demonstrated that the mature protein $OmcZ_S$ can be found in the outer membrane and cell debris fractions but not in the periplasmic or cytoplasmic fraction. The recovery of some $OmcZ_L$, but not $OmcZ_S$, in the periplasm suggests that $OmcZ_L$ is cleaved during secretion across the outer membrane, as has been reported for the secretion of other outer-surface proteins in other microorganisms (55).

Purification of $OmcZ_S$. $OmcZ_S$ was purified from the stationary-phase cells of strain ZKI because it was much more abundant than $OmcZ_L$ in these cells (Fig. 3A). It was purified by detergent extraction followed by gel filtration chromatography. After detergent extraction, the protein sample was already purified to near homogeneity (Fig. 3B). The detergent-extracted $OmcZ_S$, originally solubilized in 10% Zwittergent 3-14 solution, was poorly soluble in biochemical buffers, such as 50 mM Tris-HCl (pH 7.0), after removal of the detergent. However, detergent-extracted $OmcZ_S$ was readily soluble in pure water. Almost all of the protein stacked on top of the gel when the sample was loaded without heating (see Fig. S1A in the supplemental material). A clear $OmcZ_S$ band appeared when the sample was heated at 100°C for 5 min with SDS sample buffer (Fig. 3B). Moreover, the detergent-extracted $OmcZ_S$ was also retained on a 300-kDa-cutoff filter after centrifugation (see Fig. S1B in the supplemental material). These observations indicate that $OmcZ_S$ polymerizes or assembles with other cell constituents at this stage. To disassemble the $OmcZ_S$ into monomers, the detergent-extracted $OmcZ_S$ was

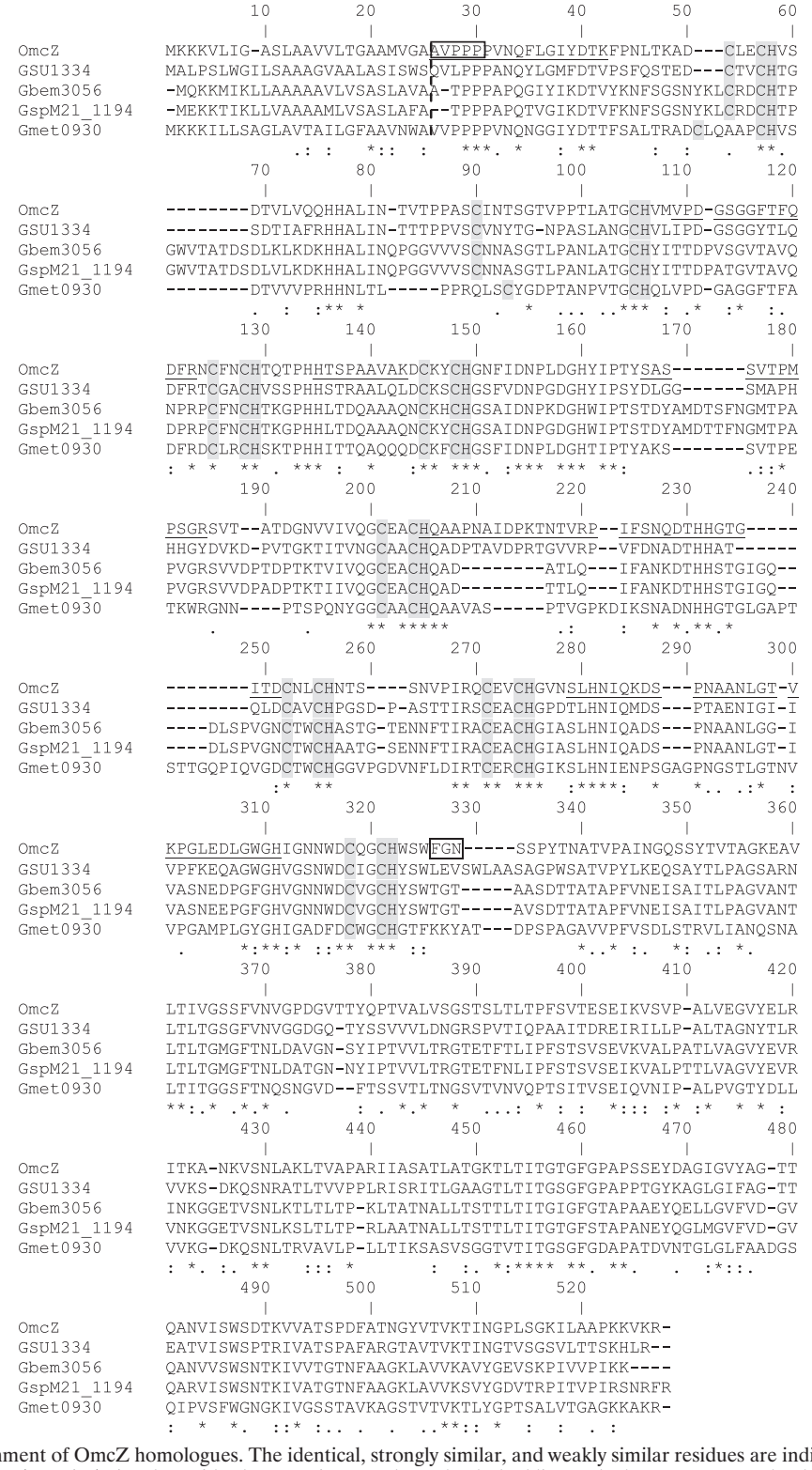

FIG. 1. Multiple alignment of OmcZ homologues. The identical, strongly similar, and weakly similar residues are indicated by asterisks, colons, and dots, respectively. The (putative) signal peptide cleavage sites are shown by dashed lines. The boxes represent the determined N terminus and C terminus sequences of $OmcZ_S$. Tryptic fragments detected by LC–MS-MS are underlined. Cysteine and histidine residues in the heme *c*-binding motifs are shaded gray.

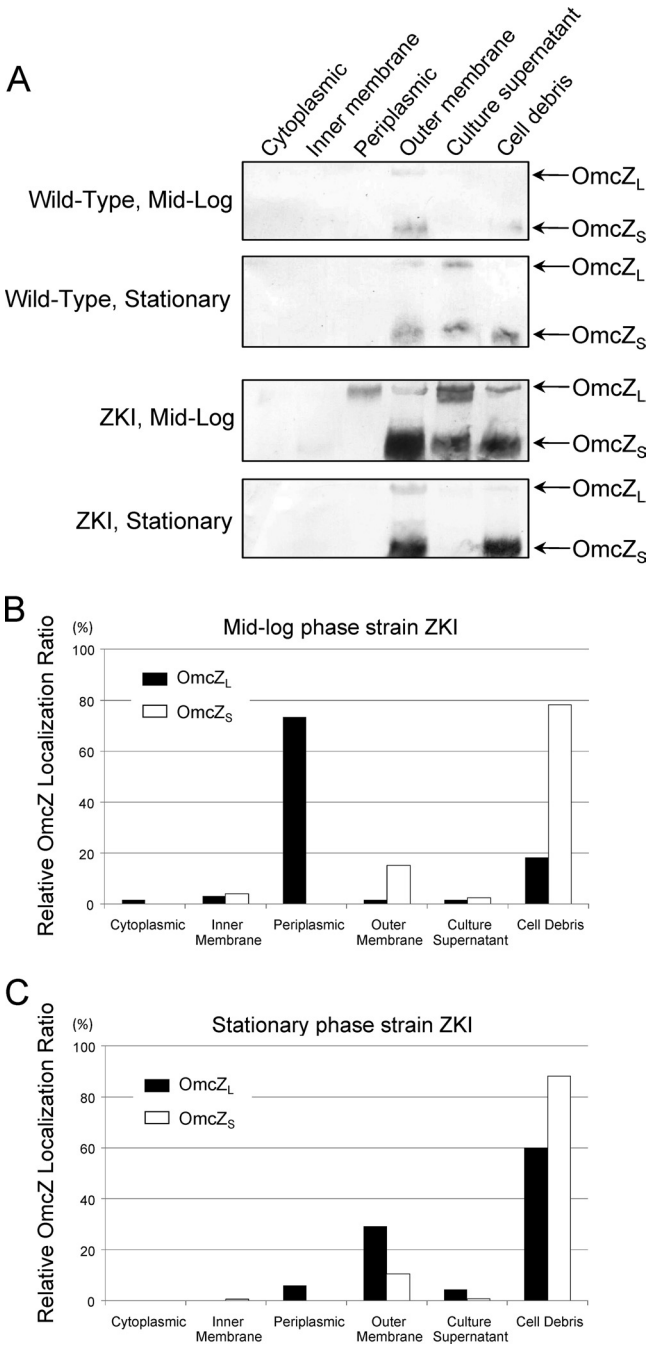

FIG. 2. Subcellular localization of $OmcZ_L$ and $OmcZ_S$ in *G. sulfurreducens* strains DL-1 and ZKI. (A) Western blot with anti-OmcZ antibody of subcellular fractions of mid-log- and stationary-phase wild-type cells and subcellular fractions of mid-log- and stationary-phase ZKI cells in acetate-fumarate culture. (B and C) Five micrograms of protein was loaded in each lane. Shown are the subcellular localization ratios of $OmcZ_L$ and $OmcZ_S$ in mid-log-phase (B) and stationary-phase (C) ZKI cells. The localization ratios were calculated using the intensities of the bands (digitized with Image J software) multiplied by total isolated protein amounts of the fractions.

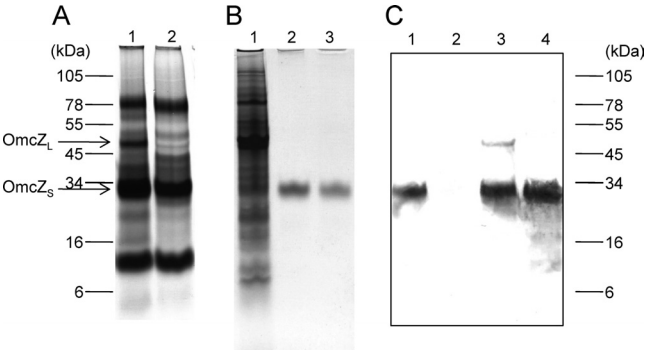

FIG. 3. $OmcZ_S$ expression (A), purification (B), and Western blot analysis (C). The proteins were separated by 12.5% Tris-Tricine denaturing polyacrylamide gel electrophoresis. (A) Heme-stained loosely bound outer membrane protein-enriched fractions from *G. sulfurreducens* strain ZKI at mid-log phase (lane 1), and stationary phase (lane 2). (B) A whole-cell sample of strain ZKI (lane 1), detergent-extracted sample (lane 2), and purified $OmcZ_S$ (lane 3) were stained with with Coomassie blue. (C) Western blot of a whole-cell sample of wild-type *G. sulfurreducens* (lane 1), an *omcZ*-deficient mutant (lane 2), a whole-cell sample of strain ZKI (lane 3), and purified $OmcZ_S$ (lane 4) using antibody against $OmcZ_S$.

heated (90°C) with 1% SDS for 5 min. After this procedure, $OmcZ_S$ passed through 300-kDa-cutoff filters (see Fig. S1B in the supplemental material).

The heat-treated sample was further purified by gel filtration chromatography. The single peak for $OmcZ_S$ was the only peak observed in the chromatograph (data not shown). The relative molecular mass of $OmcZ_S$ was calculated as 32 kDa by gel filtration chromatography. Typical yields were approximately 2 mg of protein per liter of culture. After gel filtration chromatography, the purified $OmcZ_S$ was poorly soluble in 50 mM Tris-HCl buffer but highly soluble in pure water. The purified $OmcZ_S$ in water remained on the 300-kDa-cutoff filters after centrifugation again (see Fig. S1B in the supplemental material), indicating that $OmcZ_S$ reassembled after removal of the detergents. SDS-PAGE analysis also showed self-assembling characteristics of $OmcZ_S$. The apparently dimerized and trimerized bands of the purified $OmcZ_S$ were observed when the protein sample was not heated before being loaded on the SDS-PAGE gel (see Fig. S1A in the supplemental material). SDS-PAGE and Western blotting confirmed that the final product of the purification was pure and contained a single protein band with a mass of ca. 30 kDa (Fig. 3B and C).

Physical and chemical properties of $OmcZ_S$. (i) N and C termini of $OmcZ_S$, molecular mass, and heme content. ESI-MS analysis indicated an average molecular mass of 32,582 Da for the purified $OmcZ_S$ when measured in 50% methanol and 3% acetic acid and 32,578 Da when measured under milder conditions in 10 mM ammonium bicarbonate buffer. Edman sequencing analysis of the purified $OmcZ_S$ revealed that the N terminus sequence is AVPPP, which is located 25 to 29 residues from the N terminus (Fig. 1). This indicates that the N terminus signal peptide of OmcZ is cleaved between amino acids 24 and 25, which corresponds with the cleavage site predicted by SignalP.

Digestion of the $OmcZ_S$ with carboxypeptidase Y yielded 3 amino acids: Gly (44% of the total amino acids detected [mol/mol]), Phe (33%), and Asn (19%). Among all possible sequence combinations of these 3 amino acids, GNF (136 to 138 from the N terminus) and FGN (280 to 282) were found in the

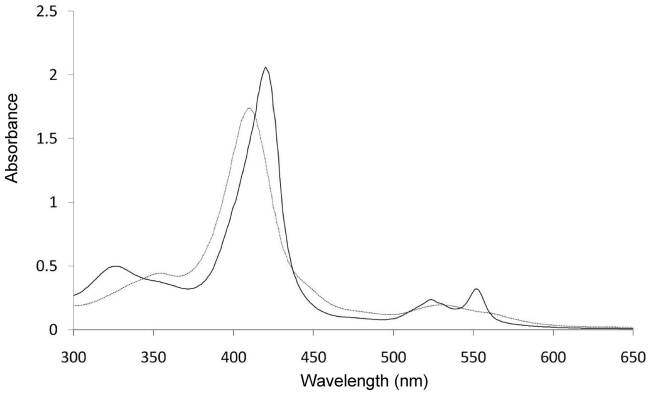

FIG. 4. UV/visible absorption spectra of $OmcZ_S$. The dotted and solid lines represent oxidized and reduced cytochrome, respectively.

OmcZ amino acid sequence. A protein with the latter C terminus gave the expected molecular mass of ca. 30 kDa.

The estimated molecular mass of $OmcZ_S$ is consistent with the predicted amino acid content (Fig. 1) and eight heme groups with a molecular mass of 616 Da. The predicted peptide sequence of $OmcZ_S$ (Fig. 1) contains all the seven predicted OmcZ heme-binding sites represented by the CXXCH motif, as well as the unusual ($CX_{14}CH$) heme-binding site. Pyridine hemochrome analysis revealed that $OmcZ_S$ contains 7.7 hemes per molecule, indicating that hemes bind to all the possible heme-binding sites.

In general, *c*-type cytochrome biogenesis in bacteria has been thought to be strictly dependent on the presence of two cysteine residues arranged in a $CX_{2-4}CH/K$ motif (16). However, the octaheme *c*-type cytochrome MccA in *Wolinella suggincogenes* contains a covalent heme attached to an unusual heme-biding $CX_{15}CH$ motif, which requires a specialized cytochrome *c* heme lyase, CcsA1, for heme attachment (16, 23). Six CcsA1-type heme lyase homologues are in the *G. sulfurreducens* genome (17), one or more of which could account for the heme incorporation into the unusual heme-binding site in OmcZ.

(ii) Thermal stability, circular dichroism (CD), and optical spectra. $OmcZ_S$ was exposed to heat (90°C) and harsh detergents, such as SDS and Zwittergent 3-14, in the purification procedure. DSC analysis of the thermal stability of $OmcZ_S$ indicated that the denaturation temperature was 94.2°C at pH 7.0.

CD spectra of purified $OmcZ_S$ demonstrated the presence of significant secondary structures. The far-UV CD spectrum indicated that $OmcZ_S$ is comprised of 13% α-helix, 18% antiparallel β-sheet, 5% parallel β-sheet, and 28% β-turn.

The UV/visible redox spectrum was characteristic of *c*-type cytochromes (Fig. 4). The maxima of the spectrum of the oxidized $OmcZ_S$ were at 408 nm (910,200 M^{-1} cm^{-1}; γ Soret band) and 530 nm (103,130 M^{-1} cm^{-1}) (Fig. 4). After reduction with DTT for 1 h, $OmcZ_S$ had absorption maxima at 419 nm (1,084,400 M^{-1} cm^{-1}; shifted γ Soret band), 523 nm (126,000 M^{-1} cm^{-1}; β Soret band), and 552 nm (171,000 M^{-1} cm^{-1}; α Soret band). These spectra are typical for *c*-type cytochromes with six coordinated low-spin hemes (2).

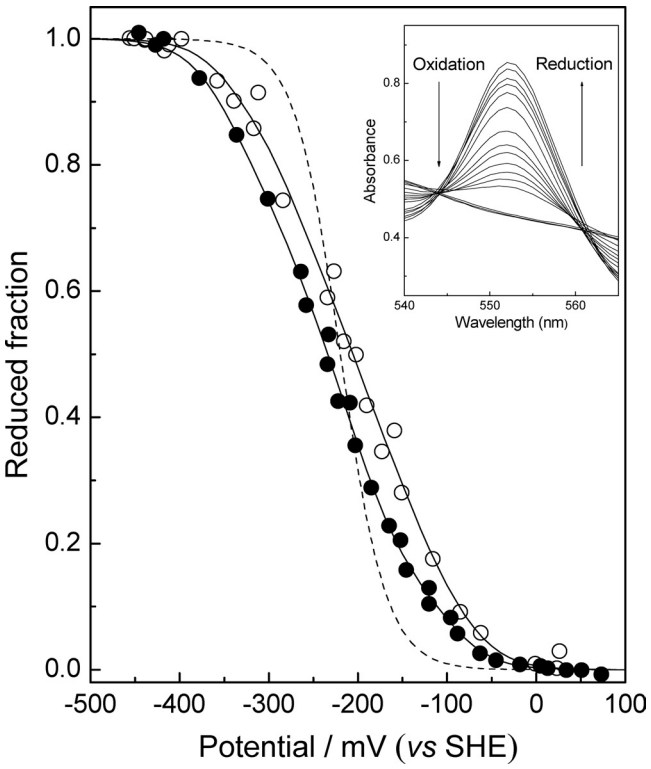

FIG. 5. Redox titrations followed by visible spectroscopy for $OmcZ_S$ at 298 K and pH 7. The open and filled symbols represent the data points in the reductive and oxidative titrations, respectively. The continuous lines indicate the fit to a model considering eight independent Nernst equations. The dashed line describes the redox curve corresponding to 8 hemes with a reduction potential of −220 mV. The inset shows the α-band region of the visible spectra used for the redox titration. In order not to overcrowd the figure, only 16 out of 54 spectra are indicated.

(iii) Redox characteristics of $OmcZ_S$. The redox behavior of OmcZs was investigated with redox titrations, followed by visible spectroscopy (Fig. 5). Both the oxidative and reductive curves spanned a large range of reduction potentials (−420 to −60 mV). The curves exhibited some hysteresis, which indicates that under these experimental conditions the protein can cycle between the fully reduced and fully oxidized states in a nonreversible way. This suggests that slowly relaxing modifications in the protein structure are associated with the redox transition. The E_{app} (i.e., the point at which the oxidized and reduced fractions are equal) values for the reductive and oxidative curve were −206 and −234 mV (versus the standard hydrogen electrode [SHE]), respectively. The shapes of the experimental curves deviate significantly from one that considers identical reduction potential values for the 8 heme groups (dashed line in Fig. 5). This observation points to nonequivalence of the redox centers, which is expected for a multiredox center protein with eight heme groups (47, 57), as is the case for $OmcZ_S$.

The large potential range of OmcZ (−420 to −60 mV versus SHE) can most probably be attributed to the wide range of the redox potentials for the 8 hemes in the molecule. This is similar to the decaheme *c*-type outer-surface cytochrome MtrC of *S. oneidensis*, which has a potential range of −500 to +100 mV

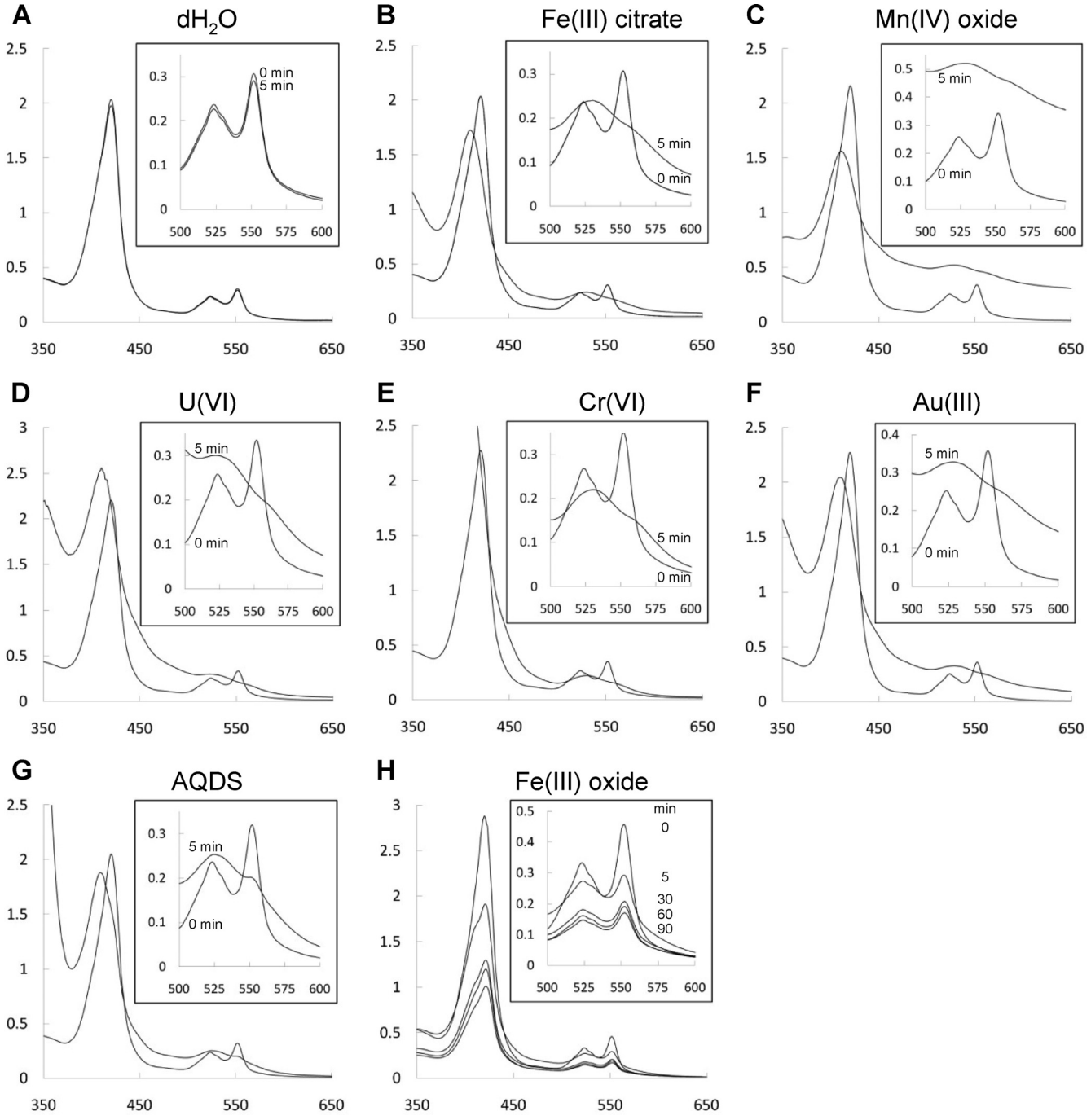

FIG. 6. Reduction of metals and AQDS with reduced $OmcZ_S$. Distilled water (dH_2O) (negative control) (A), Fe(III) citrate (B), Mn(IV) (C), U(VI) (D), Cr(VI) (E), Au(III) (F), AQDS (G), and Fe(III) oxide (H) were added to reduced $OmcZ_S$. (A to G) The UV/visible spectra 0 and 5 min after the electron acceptor candidates were added.

(15). The potential range of OmcZ covers the lowest anode potential observed in microbial fuel cells of *G. sulfurreducens* (−420 mV versus Ag/AgCl, approximately equal to −220 mV versus SHE) (5), suggesting that OmcZ has a low enough potential to directly transfer electrons to the anode.

(iv) Electron acceptors. Spectrophotometric analysis revealed that $OmcZ_S$ is rapidly (less than 5 min) oxidized with known electron acceptors for *G. sulfurreducens*, such as Fe(III) citrate, Mn(IV) oxide, U(VI), Cr(VI), Au(III), and the humic acid analogue AQDS (Fig. 6). $OmcZ_S$ was only partially reoxidized when it was incubated with Fe(III) oxide (Fig. 6H). Even after 90 min of incubation, the 419-nm γ-band did not completely shift to 408 nm (Fig. 6H, inset), indicating that $OmcZ_S$ has little activity toward Fe (III) oxide. After the addition of Fe(III) oxide, all the peaks decreased with time, probably because $OmcZ_S$ attached to the insoluble Fe(III) oxide.

Previous studies have suggested that *c*-type cytochromes are involved in the reduction of a variety of metals and the humic acid analogue AQDS by *Geobacter* spp. (25, 30–32, 37, 49, 58). The ability of OmcZ to transfer electrons to metals and AQDS, coupled with its extracellular location, suggests that OmcZ could play a role in electron transfer to these extracellular electron acceptors. The finding that OmcZ did not readily transfer electrons to insoluble Fe(III) oxide is consistent with the fact that deleting the gene for OmcZ did not have any impact on the capacity for Fe(III) oxide reduction by *G. sulfurreducens* (39). OmcZ could reduce Mn(IV) oxide quickly, but not Fe(III) oxide. This might be explained by the fact that the midpoint potential of Mn(IV) oxide is much higher (from 500 to 600 mV at 25°C, pH 7 [54]) than that of OmcZ (−220 mV), whereas the midpoint potential of Fe(III) oxide (−300 to 0 mV [54]) is comparable to that of OmcZ.

Implications. Several of the characteristics of OmcZ reported here are consistent with the requirement for OmcZ for optimal current production by *G. sulfurreducens* (39) and electrochemical results (48) that suggest that OmcZ aids in electron conduction from *G. sulfurreducens* biofilms to the anodes of microbial fuel cells. The results demonstrate that OmcZ is primarily localized in the extracellular matrix, as would be expected for a protein contributing to electron conduction in biofilms. Precedents for extracellular localization of *c*-type cytochromes include the presence of the cytochromes MtrC and OmcA in the polymeric substance surrounding cells of *S. oneidensis* (36) and recovery of a *c*-type cytochrome in the extracellular matrix purified from *Myxococcus xanthus* (10). The tendency for OmcZ to self-assemble, coupled with its poor solubility in buffers, suggests that OmcZ would be retained within the biofilm matrix rather than lost to the external medium. Therefore, the energy commitment to produce OmcZ to promote electron transfer through the biofilm is not likely to be dissipated in loss of OmcZ to the external medium. The multiple redox potentials of the hemes in OmcZ seem well suited to promoting electron transfer to anode biofilms, which may function at different potentials, depending on the resistance to electron flow and the rates of metabolism in microbial fuel cells. Studies are now under way to purify OmcS, another abundant outer-surface *c*-type cytochrome of *G. sulfurreducens* that is required for Fe(III) oxide reduction but not for high-density current production, in order to compare biochemical features that differentiate the functions of outer-surface cytochromes.

ACKNOWLEDGMENTS

This work was supported by the Office of Science (BER), U.S. Department of Energy, Cooperative Agreement no. DE-FC02-02ER63446, by Office of Naval Research award no. N00014-10-1-0084, and by Fundação para a Ciência e a Tecnologia (Portugal) research grant PTDC/BIA-PRO/74498/2006. K. Inoue is a recipient of a Japan Society for the Promotion of Science Postdoctoral Fellowship for Research Abroad. L. Morgado is supported by Fundação para a Ciência e a Tecnologia (Portugal) doctoral grant SFRH/BD/37415/2007.

We thank J. Fernandez (Rockefeller University Protein/DNA Technology Center) for the Edman sequencing analysis; S. J. Eyles (University of Massachusetts Core Mass Spectrometry Facility) for ESI-MS analysis; J. Leszyk (University of Massachusetts Medical School) for LC–MS-MS analysis; J. Nakamura, M. Uozaki, and Y. Sakaguchi (DKSH, Japan) and E. Katoh (National Institute of Agrobiological Sciences, Japan) for the DSC measurements; and T. Arakawa (Alliance Protein Laboratories) for far-UV CD analysis. We are grateful for technical support from B. Blunt and J. Ward.

REFERENCES

1. **Bartsch, R. G.** 1971. Cytochromes: bacterial. Methods Enzymol. **23:**344–363.
2. **Berry, E. A., and B. L. Trumpower.** 1987. Simultaneous determination of hemes *a*, *b*, and *c* from pyridine hemochrome spectra. Anal. Biochem. **161:** 1–15.
3. **Böhm, G., R. Muhr, and R. Jaericke.** 1992. Quantitative analysis of protein far UV circular dichroism spectra by neural networks. Protein Eng. **5:**191–195.
4. **Bond, D. R., D. E. Holmes, L. M. Tender, and D. R. Lovley.** 2002. Electrode-reducing microorganisms that harvest energy from marine sediments. Science **295:**483–485.
5. **Bond, D. R., and D. R. Lovley.** 2003. Electricity production by *Geobacter sulfurreducens* attached to electrodes. Appl. Environ. Microbiol. **69:**1548–1555.
6. **Bradford, M. M.** 1976. A rapid and sensitive method for the quantitation of microgram quantities of protein utilizing the principle of protein-dye binding. Anal. Biochem. **72:**248–254.
7. **Caccavo, F., Jr., D. J. Lonergan, D. R. Lovley, M. Davis, J. F. Stolz, and M. J. McInerney.** 1994. *Geobacter sulfurreducens* sp. nov., a hydrogen- and acetate-oxidizing dissimilatory metal-reducing microorganism. Appl. Environ. Microbiol. **60:**3752–3759.
8. **Coppi, M. V., C. Leang, S. J. Sandler, and D. R. Lovley.** 2001. Development of a genetic system of *Geobacter sulfurreducens*. Appl. Environ. Microbiol. **67:**3180–3187.
9. **Coppi, M. V., R. A. O'Neil, C. Leang, F. Kaufmann, B. A. Methé, K. P. Nevin, T. L. Woodard, A. Liu, and D. R. Lovley.** 2007. Involvement of *Geobacter sulfurreducens* SfrAB in acetate metabolism rather than intracellular, respiration-linked Fe(III) citrate reduction. Microbiology **153:**3572–3585.
10. **Curtis, P. D., J. Atwood III, R. Orlando, and L. J. Shimkets.** 2007. Proteins associated with the *Myxococcus xanthus* extracellular matrix. J. Bacteriol. **189:**7634–7642.
11. **Ding, Y. H. R., K. K. Hixson, M. A. Aklujkar, M. S. Lipton, R. D. Smith, D. R. Lovley, and T. Mester.** 2008. Proteome of *Geobacter sulfurreducens* grown with Fe(III) oxide or Fe(III) citrate as the electron acceptor. Biochim. Biophys. Acta **1784:**1935–1941.
12. **Ding, Y. H. R., K. K. Hixson, C. S. Giometti, A. S. A. Esteve-Núñez, T. Khare, S. L. Tollaksen, W. Zhu, J. N. Adkins, M. S. Lipton, R. D. Smith, T. Mester, and D. R. Lovley.** 2006. The proteome of dissimilatory metal-reducing microorganism *Geobacter sulfurreducens* under various growth conditions. Biochim. Biophys. Acta **1764:**1198–1206.
13. **Esteve-Núñez, A., J. Sosnik, P. Visconti, and D. R. Lovley.** 2008. Fluorescent properties of *c*-type cytochromes reveal their potential role as an extracytoplasmic electron sink in *Geobacter sulfurreducens*. Environ. Microbiol. **10:** 497–505.
14. **Francis, R. T., Jr., and R. R. Becker.** 1984. Specific indication of hemoproteins in polyacrylamide gels using a double-staining process. Anal. Biochem. **136:**509–514.
15. **Hartshorne, R. S., B. N. Jepson, T. A. Clarke, S. J. Field, J. Fredrickson, J. Zachara, L. Shi, J. N. Butt, and D. J. Richardson.** 2007. Characterization of *Shewanella oneidensis* MtrC: a cell-surface decaheme cytochrome involved in respiratory electron transport to extracellular electron acceptors. J. Biol. Inorg. Chem. **12:**1083–1094.
16. **Hartshorne, R. S., M. Kern, B. Meyer, T. A. Clarke, M. Karas, D. J. Richardson, and J. Simon.** 2007. A dedicated haem lyase is required for the maturation of a novel bacterial cytochrome *c* with unconventional covalent haem binding. Mol. Microbiol. **64:**1049–1060.
17. **Hartshorne, R. S., D. J. Richardson, and J. Simon.** 2006. Multiple haem lyase genes indicate substrate specificity in cytochrome *c* biogenesis. Biochem. Soc. Trans. **34:**146–149.
18. **Holmes, D. E., D. R. Bond, R. A. O'Neil, C. E. Reimers, L. R. Tender, and D. R. Lovley.** 2004. Microbial communities associated with electrodes harvesting electricity from a variety of aquatic sediments. Microb. Ecol. **48:**178–190.
19. **Ishii, S., K. Watanabe, S. Yabuki, B. E. Logan, and Y. Sekiguchi.** 2008. Comparison of electrode reduction activities of *Geobacter sulfurreducens* and an enriched consortium in an air-cathode microbial fuel cell. Appl. Environ. Microbiol. **74:**7348–7355.
20. **Jung, S., and J. M. Regan.** 2007. Comparison of anode bacterial communities and performance in microbial fuel cells with different electron donors. Appl. Microbiol. Biotechnol. **77:**393–402.
21. **Kaufmann, F., and D. R. Lovley.** 2001. Isolation and characterization of a soluble NADPH-dependent Fe(III) reductase from *Geobacter sulfurreducens*. J. Bacteriol. **183:**4468–4476.
22. **Kim, B.-C., C. Leang, Y. H. R. Ding, R. H. Glaven, M. V. Coppi, and D. R. Lovley.** 2005. OmcF, a putative *c*-type monoheme outer membrane cytochrome required for the expression of other outer membrane cytochromes in *Geobacter sulfurreducens*. J. Bacteriol. **187:**4505–4513.
23. **Kranz, R. G., C. Richard-Fogal, J. S. Taylor, and E. R. Frawley.** 2009. Cytochrome *c* biogenesis: mechanisms for covalent modifications and traf-

ficking of heme and for heme-iron redox control. Microbiol. Mol. Biol. Rev. **73:**510–528.
24. **Leang, C., L. A. Adams, K. J. Chin, K. P. Nevin, B. A. Methé, J. Webster, M. L. Sharma, and D. R. Lovley.** 2005. Adaptation to disruption of the electron transfer pathway for Fe(III) reduction in *Geobacter sulfurreducens*. J. Bacteriol. **187:**5918–5926.
25. **Leang, C., M. V. Coppi, and D. R. Lovley.** 2003. OmcB, a *c*-type polyheme cytochrome, involved in Fe(III) reduction in *Geobacter sulfurreducens*. J. Bacteriol. **185:**2096–2103.
26. **Lee, H. S., P. Parameswaran, A. Kato-Marcus, C. I. Torres, and B. E. Rittmann.** 2008. Evaluation of energy-conversion efficiencies in microbial fuel cells (MFCs) utilizing fermentable and non-fermentable substrates. Water Res. **42:**1501–1510.
27. **Liu, Y., F. Harnisch, K. Fricke, R. Sietmann, and U. Schröder.** 2008. Improvement of the anodic bioelectrocatalytic activity of mixed culture biofilms by a simple consecutive electrochemical selection procedure. Biosens. Bioelectron. **24:**1012–1017.
28. **Lloyd, J. R., C. Leang, A. L. Hodges-Myerson, M. V. Coppi, S. Cuifo, B. Methe, S. J. Sandler, and D. R. Lovley.** 2003. Biochemical and genetic characterization of PpcA, a periplasmic *c*-type cytochrome in *Geobacter sulfurreducens*. Biochem. J. **369:**153–161.
29. **Louro, R. O., T. Catarino, J. LeGall, D. L. Turner, and A. V. Xavier.** 2001. Cooperativity between electrons and protons in a monomeric cytochrome c_3: the importance of mechano-chemical coupling for energy transduction. Chembiochem **2:**831–937.
30. **Lovley, D. R.** 1993. Dissimilatory metal reduction. Annu. Rev. Microbiol. **47:**263–290.
31. **Lovley, D. R., J. D. Coates, E. L. Blunt-Harris, E. J. P. Phillips, and J. C. Woodward.** 1996. Humic substances as electron acceptors for microbial respiration. Nature **382:**445–448.
32. **Lovley, D. R., S. J. Giovannoni, D. C. White, J. E. Champine, E. J. P. Phillips, Y. A. Gorby, and S. Goodwin.** 1993. *Geobacter metallireducens* gen. nov. sp. nov., a microorganism capable of coupling the complete oxidation of organic compounds to the reduction of iron and other metals. Arch. Microbiol. **159:**336–344.
33. **Lovley, D. R., E. J. P. Phillips, Y. A. Gorby, and E. R. Landa.** 1991. Microbial reduction of uranium. Nature **350:**413–416.
34. **Magnuson, T. S., L. H. M. Allison, and D. R. Lovley.** 2000. Characterization of a membrane-bound NADH-dependent Fe^{3+} reductase from the dissimilatory Fe^{3+}-reducing bacterium *Geobacter sulfurreducens*. FEMS Microbiol. Lett. **185:**205–211.
35. **Magnuson, T. S., N. Isoyama, A. L. Hodges-Myerson, G. Davidson, M. J. Maroney, G. G. Geesey, and D. R. Lovley.** 2001. Isolation, characterization and gene sequence analysis of a membrane-associated 89 kDa Fe(III) reducing cytochrome *c* from *Geobacter sulfurreducens*. Biochem. J. **359:**147–152.
36. **Marshall, M. J., A. S. Beliaev, A. C. Dohnalkova1, D. W. Kennedy, L. Shi, Z. Wang, M. I. Boyanov, B. Lai, K. M. Kemner, J. S. McLean, S. B. Reed, D. E. Culley, V. L. Bailey, C. J. Simonson, D. A. Saffarini, M. F. Romine, J. M. Zachara, and J. K. Fredrickson.** 2006. *c*-Type cytochrome-dependent formation of U(IV) nanoparticles by *Shewanella oneidensis*. PLoS Biol. **4:**1324–1333.
37. **Mehta, T., M. V. Coppi, S. E. Childers, and D. R. Lovley.** 2005. Outer membrane *c*-type cytochromes required for Fe(III) and Mn(IV) oxide reduction in *Geobacter sulfurreducens*. Appl. Environ. Microbiol. **71:**8634–8641.
38. **Morgado, L., M. Bruix, V. Orshonsky, Y. Y. Londer, N. E. C. Duke, X. Yang, P. R. Pokkuluri, M. Schiffer, and C. A. Salgueiro.** 2008. Structural insights into the modulation of the redox properties of two *Geobacter sulfurreducens* homologous triheme cytochromes. Biochim. Biophys. Acta **1777:**1157–1165.
39. **Nevin, K. P., B.-C. Kim, R. H. Glaven, J. P. Johnson, T. L. Woodard, B. A. Methé, R. J. DiDonato, Jr., S. F. Covalla, A. E. Franks, A. Liu, and D. R. Lovley.** 2009. Differences in physiology between current-producing and fumarate-reducing biofilms of *Geobacter sulfurreducens*: identification of a novel outer-surface cytochrome essential for electron transfer to anodes at high current densities. PLoS One **4:**e5628.
40. **Nevin, K. P., H. Richter, S. F. Covalla, J. P. Johnson, T. L. Woodard, A. L. Orloff, H. Jia, M. Zhang, and D. R. Lovley.** 2008. Power output and columbic efficiencies from biofilms of *Geobacter sulfurreducens* comparable to mixed community microbial fuel cells. Environ. Microbiol. **10:**2505–2514.
41. **Nikaido, H.** 1994. Isolation of outer membranes. Methods Enzymol. **235:**225–234.
42. **Paquete, C. M., D. L. Turner, R. O. Louro, A. V. Xavier, and T. Catarino.** 2007. Thermodynamic and kinetic characterization of individual haems in multicentre cytochromes c_3. Biochim. Biophys. Acta **1767:**1169–1179.
43. **Pessanha, M., L. Morgado, R. O. Louro, Y. Y. Londer, P. R. Pokkuluri, M. Schiffer, and C. A. Salgueiro.** 2006. Thermodynamic characterization of triheme cytochrome PpcA from *Geobacter sulfurreducens*: evidence for a role played in e^-/H^+ energy transduction. Biochemistry **45:**13910–13917.
44. **Pokkuluri, P. R., Y. Y. Londer, S. J. Wood, N. E. C. Duke, L. Morgado, C. A. Salgueiro, and M. Schiffer.** 2009. Outer membrane cytochrome *c*, OmcF, from *Geobacter sulfurreducens*: high structural similarity to an algal cytochrome c_6. Proteins **74:**266–270.
45. **Pokkuluri, P. R., M. Pessanha, Y. Y. Londer, S. J. Wood, N. E. C. Duke, R. Wilton, T. Catarino, C. A. Salgueiro, and M. Schiffer.** 2008. Structures and solution properties of two novel periplasmic sensor domains with *c*-type heme from chemotaxis proteins of *Geobacter sulfurreducens*: implications for signal transduction. J. Mol. Biol. **377:**1498–1517.
46. **Qi, Q., and W. Zimmermann.** 2005. Cyclodextrin glucanotransferase: from gene to applications. Appl. Microbiol. Biotechnol. **66:**475–485.
47. **Reis, C., R. O. Louro, I. Pacheco, T. Catarino, D. L. Turner, and A. V. Xavier.** 2002. Redox-Bohr effect in the nine haem cytochome from *Desulfovibrio desulfuricans* 27774. Inorg. Chim. Acta **339:**248–252.
48. **Richter, H., K. P. Nevin, H. Jia, D. A. Lowy, D. R. Lovley, and L. M. Tender.** 2009. Cyclic voltammetry of biofilms of wild type and mutant *Geobacter sulfurreducens* on fuel cell anodes indicates possible roles of OmcB, OmcZ, type IV pili, and protons in extracellular electron transfer. Energy Environ. Sci. **2:**506–516.
49. **Shelobolina, E. S., M. V. Coppi, A. A. Korenevsky, L. N. DiDonato, S. A. Sullivan, H. Konishi, H. Xu, C. Leang, J. E. Butler, B.-C. Kim, and D. R. Lovley.** 2007. Importance of *c*-type cytochromes for U(VI) reduction by *Geobacter sulfurreducens*. BMC Microbiol. **7:**16.
50. **Shi, L., D. J. Richardson, Z. Wang, S. N. Kerisit, K. M. Rosso, J. M. Zachara, and J. K. Fredrickson.** 2009. The roles of outer membrane cytochromes of *Shewanella* and *Geobacter* in extracellular electron transfer. Environ. Microbiol. Rep. **1:**220–227.
51. **Shi, L., T. C. Squier, J. M. Zachara, and J. K. Fredrickson.** 2007. Respiration of metal (hydr)oxides by *Shewanella* and *Geobacter*: a key role for multihaem *c*-type cytochromes. Mol. Microbiol. **65:**12–20.
52. **Smith, P. K., R. I. Krohn, G. T. Hermanson, A. K. Mallia, F. H. Gartner, M. D. Provenzano, E. K. Fujimoto, N. M. Goeke, B. J. Olson, and D. C. Klenk.** 1985. Measurement of protein using bicinchonic acid. Anal. Biochem. **150:**76–85.
53. **Tender, L. M., C. E. Reimers, H. A. Stecher III, D. A. Holmes, D. R. Bond, D. A. Lowy, K. Pilobello, S. J. Fertig, and D. R. Lovley.** 2002. Harnessing microbially generated power on the seafloor. Nat. Biotechnol. **20:**821–825.
54. **Thamdrup, B.** 2000. Bacterial manganese and iron reduction in aquatic sediments. Adv. Microb. Ecol. **16:**41–84.
55. **Thanassi, D. G., and S. J. Hultgren.** 2000. Multiple pathways allow protein secretion across the bacterial outer membrane. Curr. Opin. Cell Biol. **12:**420–430.
56. **Thomas, P. E., D. Ryan, and W. Levin.** 1976. An improved staining procedure for the detection of the peroxidase activity of cytochrome P-450 on sodium dodecyl sulfate polyacrylamide gels. Anal. Biochem. **75:**168–176.
57. **Valente, F. M. A., L. M. Teixeira, J. LeGall, A. V. Xavier, M. Teixeira, and I. A. C. Pereira.** 2001. A membrane-bound cytochrome c_3: a type II cytochrome c_3 from *Desulfovibrio vulgaris* Hildenborough. Chembiochem **2:**895–905.
58. **Voordeckers, J. W., B.-C. Kim, M. Izallalen, and D. R. Lovley.** 2010. Role of *Geobacter sulfurreducens* outer surface *c*-type cytochromes in reduction of soil humic acid and anthraquinone-2,6-disulfonate. Appl. Environ. Microbiol. **76:**2371–2375.
59. **Yi, H., K. P. Nevin, B.-C. Kim, A. E. Franks, A. Klimes, L. M. Tender, and D. R. Lovley.** 2009. Selection of a variant of *Geobacter sulfurreducens* with enhanced capacity for current production in microbial fuel cells. Biosens. Bioelectron. **24:**3498–3503.